ELSEVIER

Ceramics International 31 (2005) 361–369

CERAMICS INTERNATIONAL

www.elsevier.com/locate/ceramint

Correlation of the physico chemical properties of Zn-substituted Li–La ferrite

M.A. Ahmed[a,*], N. Okasha[b], A. Ebrahem[c]

[a]*Physics Department, Faculty of Science, Cairo University, Giza, Egypt*
[b]*Physics Department, Faculty of Girls, Ain Shams University, Cairo, Egypt*
[c]*Physics Department, Institute of Applied Physics, Yonsei University, Seoul, Korea*

Received 11 February 2004; received in revised form 3 March 2004; accepted 3 May 2004
Available online 30 December 2004

Abstract

The electrical resistivity, magnetic susceptibility, and the thermoelectric power of Zn-substituted Li–La mixed ferrite with formula $Li_{0.5-0.5x}Zn_xLa_yFe_{2.5-0.5x-y}O_4$ at $0.1 \leq x \leq 0.9$; $y = 0.04$ were studied as a function of temperature and frequency. X-ray analysis and Seebeck coefficient measurement were carried out in order to assure the formation of the sample in single spinel phase and to know the type of charge carriers participating in the conduction mechanism. The dependence of the electrical resistivity of Li–Zn ferrite on Zn content and temperature is explained on the basis of the cation distribution. The transition from the ferromagnetic to paramagnetic state is accompanied by an increase in the thermo EMF. Li–Zn ferrite shows n- and p-types conductivity due to the presence of Fe^{2+} ions. The creation of lattice vacancies is due to the presence of Li ions which give rise of p-type conductivity.

Keywords: C. Electrical properties; C. Magnetic properties; D. Ferrites; Thermoelectric power; Li–Zn–La ferrites

1. Introduction

Li–Zn ferrite is one of the ideal inverse spinel structures [1]. This structure consists of a cubic-closed packed cage of oxygen ions with the metallic ions occupying the tetrahedral (A) and the octahedral (B) interstitial sites, which interact with each other through the super exchange interactions J_{AA}, J_{AB} and J_{BB} with $J_{AB} > J_{BB} > J_{AA}$. Magnetic disorder can be easily introduced into the system by either selective sublattice dilution or cation distribution.

Lithium ferrites are low cost materials which are generally having vast applications from microwave to radio frequency region [2]. The low electrical conductivity resulting in low losses makes this type of ferrite attractive materials especially for microwave applications. The order of magnitude of the conductivity greatly influences the electric and magnetic behavior of ferrites where the spinel lithium ferrite contains Fe^{2+} and lithium ions and therefore it is expected that this material exhibits both electronic and ionic conductivities [3]. The modifications of the different properties of ferrites due to the substitution of divalent, trivalent and tetravalent ions have been studied by several authors [4,5].

Lithium–zinc ferrite is a pertinent magnetic material for applications because of its better properties at high frequency and lower densification temperatures than other ferrites. It is well known that the intrinsic parameters of the high frequency lithium–zinc depend on composition, technological factors and additive or substitutions as well as the other preparation conditions. The reduction of porosity is a problem in Li–Zn ferrite because the lithium volatility and oxygen loss imply a limitation on the sintering temperature. By introducing a relatively small amount of foreign ions an important modification of both structure and magnetic properties can be obtained [6,7].

By introducing nonmagnetic ions such as Zn^{2+} in Li–ferrite a very large influence on several of its magnetic properties such as magnetization, magnetic susceptibility, Curie temperature, etc. takes place. Zn^{2+} ion also has

* Corresponding author.
E-mail address: moala47@hotmail.com (M.A. Ahmed).

0272-8842/$30.00
doi:10.1016/j.ceramint.2004.05.017

considerable effect on other properties of lithium ferrite like B-site ordering, dielectric behavior, electrical resistivity, etc. [8].

D. Ravinder [9] and P.V. Reddy et al. [10] studied the behavior of the thermoelectric power in the neighborhood of T_C for Li–Zn ferrite to get an insight into the mechanism of charge transport behavior.

The aim of the present work is to study the effect of replacement of divalent Zn^{2+} ions on the electrical, magnetic, thermoelectric power and structural properties of Li–La ferrite.

2. Experimental

Polycrystalline solid solution of $Li_{0.5-0.5x}Zn_xLa_{y}Fe_{2.5-0.5x-y}O_4$ samples; $0.1 \leq x \leq 0.9$ and $y = 0.04$ were prepared by the standard ceramic technique [11] using high purity oxides of Fe_2O_3, ZnO, LiOH and La_2O_3 from British Drug House (BDH). Stoichiometric ratios are mixed, well grounded and presintered at 600 °C for 8 h, then grinded again and presintered another time at 600 °C for 15 h. The samples were pressed into pellets form under a pressure of 1.9×10^8 N/m^2 and finally sintered at 1150 °C for 10 h followed by cooling to room temperature with the same rate as that of heating (4 °C/min) in the Lenton furnace 16/5 UAF (England). Some of the samples were crushed again in an agate mortar to fine powder for magnetic susceptibility measurement and the two surfaces of the other pellets were polished to obtain a uniform thickness and coated with silver paste as a good Ohmic contact surface.

The completion of the reaction and production of single phase material at room temperature was verified by Scintag (USA) X-ray diffractometer equipped with Cu Kα (λ = 1.5418 °A) radiation source with nickel filter. X-ray pattern as in Fig. 7 indicate the crystalline phase belonging to the face center cubic (fcc) system. The magnetic interactions of the spinel system were calculated from dc magnetic susceptibility measurements using Faraday's method in which the sample was inserted at the point of maximum gradient. The measurements were performed over a temperature range where a paramagnetic behavior was observed in all the samples.

The real part of dielectric constant (ε') and ac electrical conductivity ($\ln \sigma_{ac}$) were measured using Hioki LCR high tester 3531 (Japan) at different temperatures (300–800 K) as a function of frequency (40 kHz–2 MHz). The values of ε' were calculated from the capacitance (c) using the formula $\varepsilon' = cd/\varepsilon_o A$, where d is the thickness of the sample, A is the cross-sectional area of the flat surface of the pellet and ε_o is the free-space permittivity. The temperature of the samples was measured using K-type thermocouple with junction in contact with the sample to obtain the exact temperature with

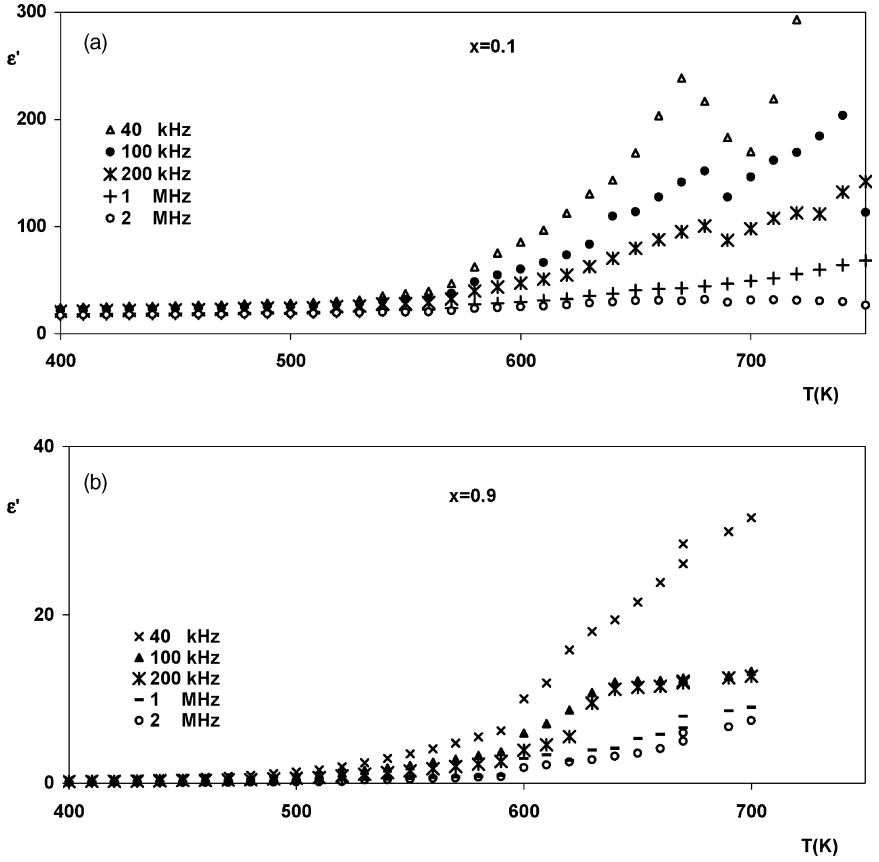

Fig. 1. (a and b) Dependence of ε' on the absolute temperature T (K) as a function of frequency at different Zn content (x).

accuracy better than ± 1 °C. The thermoelectric power measurements (Seebeck coefficient) as a function of temperature were measured across the pellet to determine the type of charge carriers.

3. Results and discussion

3.1. Electrical properties

Fig. 1(a) and (b) is a typical curve showing the relation between the real part of dielectric constant (ε') and absolute temperature (T) from 300 to 800 K as a function of the applied frequency ranging from 40 kHz to 2 MHz. It can be seen from the figure that the value of ε' decreases continuously with increasing frequency without any change in the Curie temperature (T_C) with increasing frequency. This reduction of ε' occurs because beyond a certain frequency of the externally applied electric field, the electronic exchange between ferrous and ferric ions, i.e. $Fe^{2+} \leftrightarrow Fe^{3+} + e^-$ is fast and the formed dipoles cannot follow the field variations. This behavior of ε' is explained qualitatively by the assumption that the mechanism of polarization and conduction processes are of the same origin. A similar temperature variation of the dielectric constant has been reported earlier [12–14].

Fig. 2(a) and (b) shows the variation of $\ln \sigma$ ($S\,cm^{-1}$), where $S = \Omega^{-1}$ (Simon) with 1000 T^{-1} (K^{-1}) for the samples under investigated. The behavior is similar to that of similar ferrites with a change in the slopes of the straight lines at a

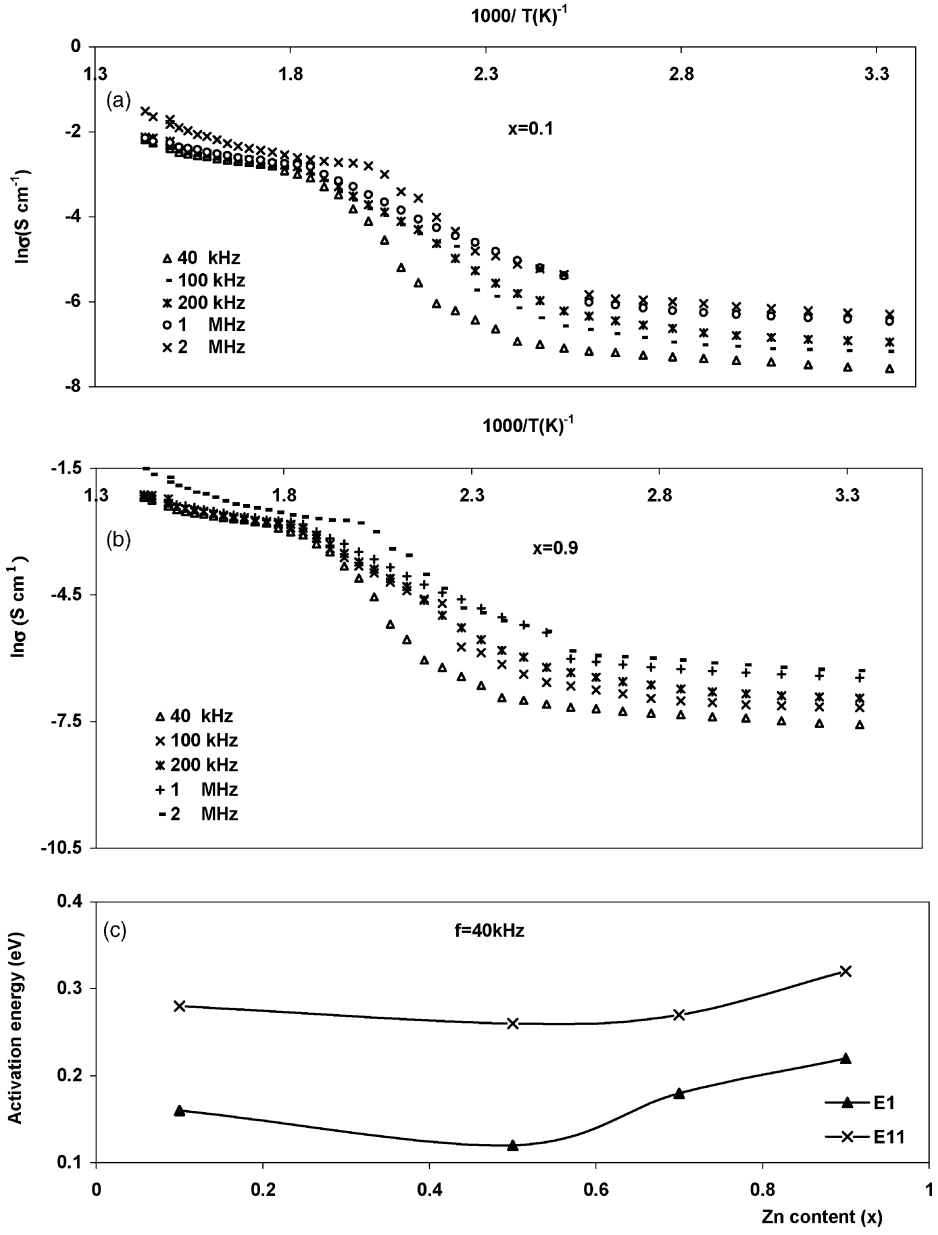

Fig. 2. (a and b) The relation between the electrical conductivity ($\ln \sigma$) and 1000 T^{-1} (K^{-1}) at different frequency.

Table 1
Activation energy values in the low (E_1) and high (E_{11}) regions at different Zn content (x) of $Li_{0.5-0.5x}Zn_xLa_yFe_{2.5-0.5x-y}O_4$

Zn content (x)	40 kHz		100 kHz		200 kHz		1000 kHz		2000 kHz	
	E_1	E_{11}	E_1	E_{11}	E_1	E_{11}	E_1	E_{11}	E_1	E_{11}
0.1	0.16	0.28	0.2	0.38	0.18	0.39	0.13	0.32	0.12	0.22
0.5	0.12	0.26	0.24	0.28	0.11	0.25	0.15	0.22	0.14	0.23
0.7	0.18	0.27	0.2	0.24	0.17	0.25	0.15	0.23	0.13	0.22
0.9	0.22	0.32	0.18	0.35	0.15	0.32	0.11	0.28	0.12	0.25

certain temperature which corresponds to the Curie temperature indicating the different conduction mechanisms. The activation energy of the different regions was calculated from the experimental data using the relation $\sigma = \sigma_o \exp^{(-\Delta E/kT)}$ and reported in Table 1, where ΔE represents the activation energy, σ is the conductivity at temperature T, σ_o is a temperature independent constant, and k is the Boltzman constant. From the figure it is clear that, the value of ln σ increases almost linearly with increasing temperature up to a certain temperature at which the slopes of lines are varied. This means that, the ferrimagnetic material transforms to paramagnetic at the Curie temperature. This indicates that the Li–Zn ferrite samples in this study exhibit semiconducting behavior and the values of the activation energy for electric conduction E_1 in the ferrimagnetic and E_{11} in the paramagnetic regions enhances this behavior. It is interesting to note that the value of the Curie temperature (T_C) is found to decrease continuously with increasing zinc content. This means the weakening of the AB interaction increases with zinc content which cause a decrease in the Curie temperature as mentioned by another authors in mixed Ni–Zn ferrites and Li–Zn ferrites [15–17].

Accordingly, the conduction at lower temperature region (below Curie temperature) is due to hopping of electron between Fe^{2+} and Fe^{3+} ions and holes due to replacement of small ionic radius ($r_{Li} = 0.60$ °A) of monovalent Li^{1+} ions on the expense of relatively larger Fe^{3+} ($r_{Fe^{3+}} = 0.64$ °A) on octahedral (B) site. While, at higher temperature (above Curie temperature) it is due to polaron hopping in addition to the electron hopping between iron ions of different valances which is the most predominant one in this region [18].

Fig. 3(a) and (b) shows the dependence of the dielectric constant ε' on the applied frequency at 650 K for the investigated samples. From the figure it is clear that, the decrease of ε' with increasing frequency is a general trend which is due to the scattering of charge carriers as they can

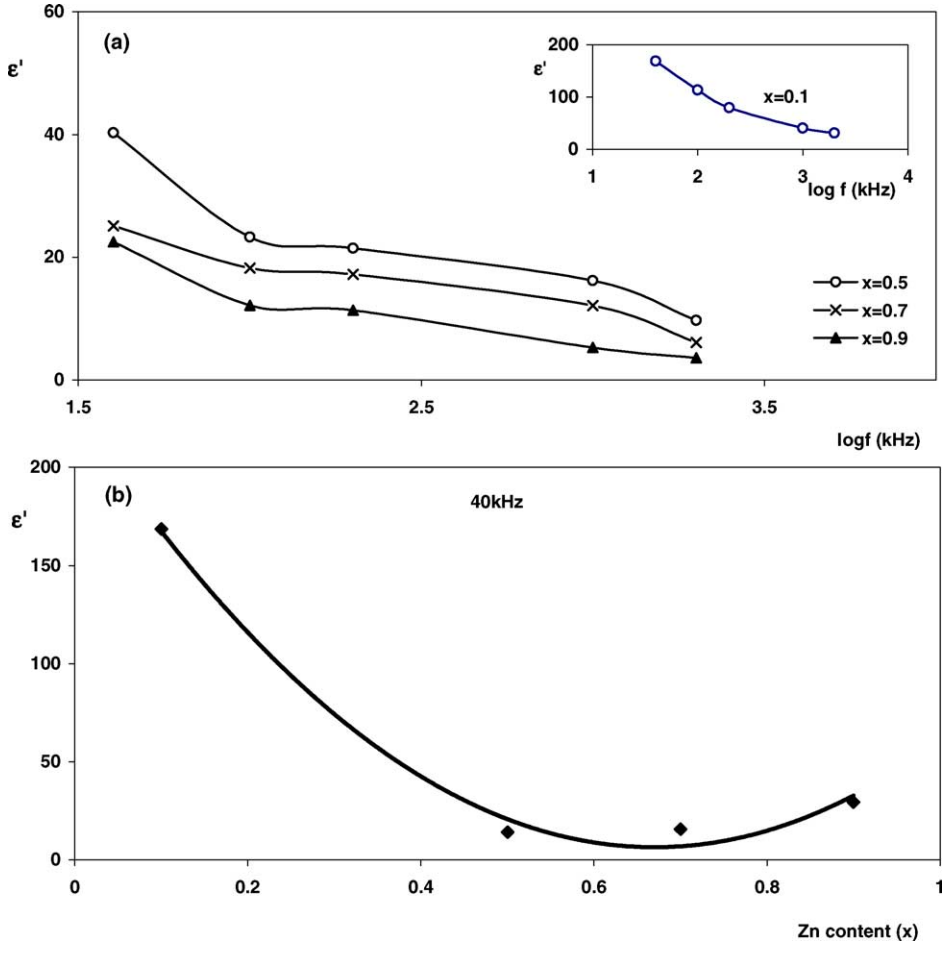

Fig. 3. (a) Dielectric constant ε' vs. frequency at different concentration ($0.1 \leq x \leq 0.9$) and selected temperature (650 K). (b) Dielectric constant ε' vs. Zn content (x) at a selected frequency (40 kHz).

not follow the fast variation of the electric field accompanied with the applied frequency. Accordingly the random orientation of the dipole moments reduces the values of ε'. Fig. 3(b) correlates the dielectric constant ε' at different Zn content (x) as a function of frequency ranging from 40 kHz to 2 MHz at 600 K. The figure indicates a decrease in ε' with increasing Zn content down to minimum value corresponding to $x = 0.5$, which is considered as the critical concentration, after which ε' increases. The presence of Fe^{3+} and Fe^{2+} simultaneously on the B-sites plays a significant role in conduction process according to the electron exchange between these two ions. While the presence of Zn^{2+} and Li^{1+} ions on A-sites makes bears p-type conduction. This means that, the two conduction processes are present and the sample is partly compensated due to the simultaneous presence of acceptor and donor centers [19]. The polarization in the tetrahedral sites is opposite to that of octahedral sites which depends on the cation distribution on both sites.

3.2. Magnetic properties

Fig. 4(a)–(d) is a typical curve correlates molar magnetic susceptibility (χ_M) and absolute temperature T (K) ranging from 300 to 900 K as a function of three selected magnetic field intensities of (2160, 3000, 3800 Oe). The data shows a normal behavior of χ_M with temperature for $x \leq 0.5$ which is similar to that of ferrimagnetic spinel ferrites. For $x > 0.5$ the existence of magnetic ordering can not be explained on the basis of paramagnetic to ferrimagnetic transition but it can be explained on the basis of the temperature evolution of the spin–spin correlation within and between groups of spins

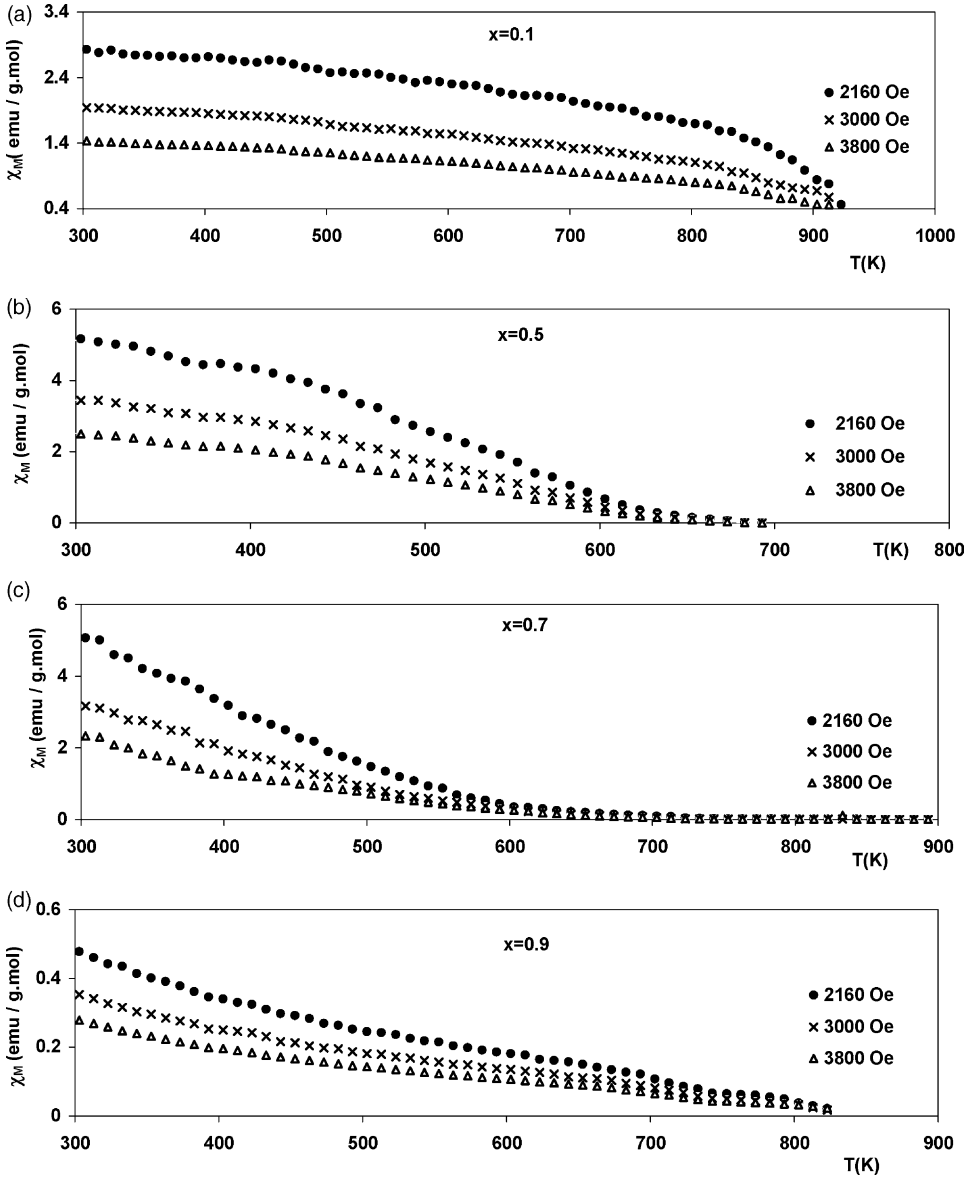

Fig. 4. (a–d) Temperature dependence of the dc magnetic susceptibility for $Li_{0.5-0.5x}Zn_xLa_yFe_{2.5-0.5x-y}O_4$ with different magnetic field intensity.

or clusters [20]. Also, as the temperature decreases gradually an increase in the magnetic susceptibility takes place at the Curie temperature (T_C) for each sample. In other words, at low temperature region (ferrimagnetic), one can deduce that, the thermal energy given to the samples is not sufficient to overcome the effect of the magnetic field which align the spins in its direction, and the result of that is the slower decrease of χ_M with increasing temperature. In the high temperature region (paramagnetic), the thermal energy due to heating increases the lattice vibration as well as the disordered state of spins and consequently overcome the field effect, causing the fast decrease in molar susceptibility.

Fig. 5(a) shows the variation of Curie temperature (T_C) with Zn content (x). It can be seen from the data that, the gradual decrease of T_C up to $x = 0.5$ where the transition takes place from ferrimagnetic to paramagnetic state and shifted to lower temperature then increases. The decrease of T_C may be due to the fact that Li–Fe interactions on the B-sites are smaller than Fe–Fe interaction [19,5]. The increase of T_C at $x \geq 0.5$ is due to the magnetic moment caused by unpaired spins only because of quenched orbital magnetic moment. Generally in case of rare earth substituted ferrites, the orbital contribution is predominant and the sample shows high magneto crystalline anisotropy. Consequently, it requires higher demagnetizing field or higher temperature to transform the material from ordered ferrimagnetic to disordered paramagnetic state. This could be the reason for the increase in the Curie temperature as in case of La^{3+} ions.

Fig. 5(b) represents the variation of the effective magnetic moment (μ_{eff}) with Zn content (x) as a function of applied magnetic field for the investigated samples. From the figure it is clear that, the effective magnetic moment decreases with increasing Zn content up to the critical concentration (x = 0.5). This increase can be explained on the basis of cation distribution between octahedral and tetrahedral sites [1]. At lowest Zinc content ($x = 0.1$), the preferences of Zn ions on tetrahedral [21] sites is maximum, while Fe^{3+} and Li^{1+} ions occupancy on octahedral sites is minimum. This leads to a smaller magnetic moment of the tetrahedral sites than that of the octahedral sites. It is known that, the magnetic moment of ferrite samples are relatively high due to antiferromagnetic coupling between A- and B-sites, the lower values of magnetic moment as in Fig. 5(b) are attributed to the presence of some of La^{3+} ions on B-sites. Thereby decreasing the number of Fe^{3+} ions. This means that, the total magnetic moment is equal the difference in moments between B and A sublattices which leads to large values of the effective magnetic moment. With increasing Zn content after $x = 0.5$ on the expense of Li^{1+} ions on A-sites,

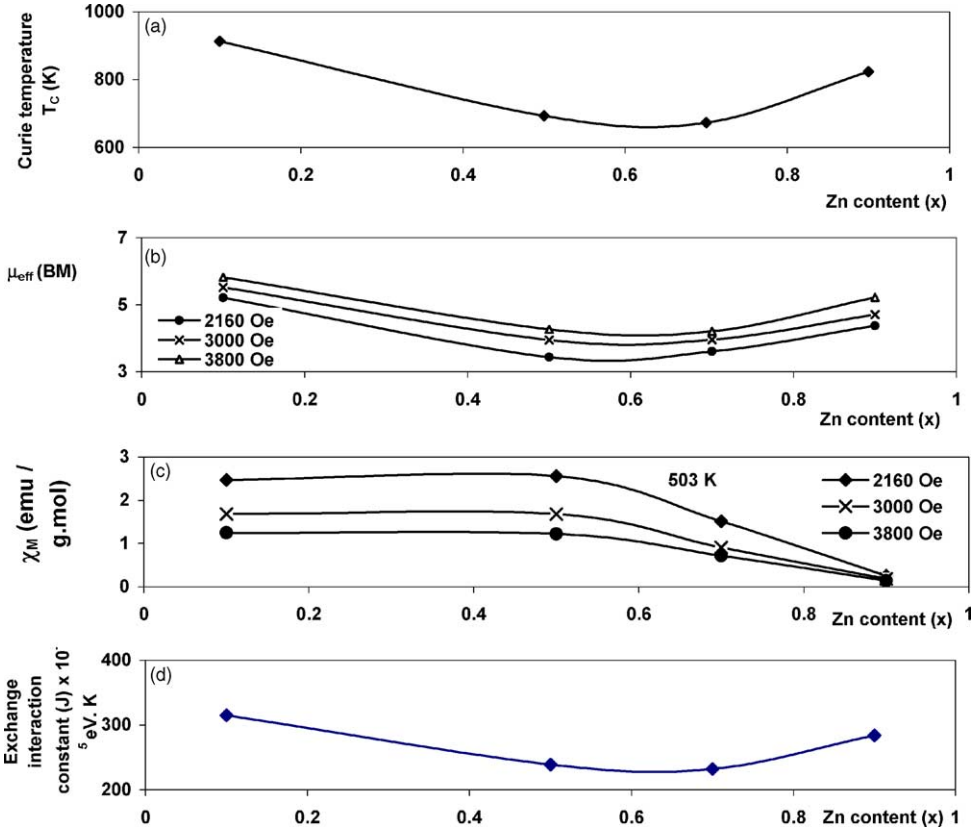

Fig. 5. (a) The values of Curie temperature (T_C) as a function of Zn content (x). (b) Dependence of the effective magnetic moment μ_{eff} on Zn content (x) at different magnetic field intensity. (c) Molar magnetic susceptibility χ_M depending on Zn content (x) at different magnetic field intensity. (d) The relation between exchange interaction (J) and Zn content (x).

rearrangement of cations in the sublattices takes place and some of Fe^{3+} ions migrate from A-sites to B-sites with the result of increasing the magnetic moment of B-sites.

Fig. 5(c) shows the variation of the molar magnetic susceptibility (χ_M) with Zn content as a function of the magnetic field intensity (2160, 3000 and 3800 Oe) at 503 K. The data gives nearly stable values of (χ_M) up to the critical concentration ($x = 0.5$) and then decreases. This behavior is due to the different exchange interaction between A and B sublattices as a result of the replacement of Fe^{2+} which comes from Fe^{3+} on the expense of Zn^{2+} on tetrahedral sites as mentioned before.

3.3. Seebeck voltage coefficient and structural properties

Fig. 6(a)–(d) clarifies the temperature dependence of Seebeck coefficient (S) for the investigated samples. From the figure it is clear that, the values of S at $x \leq 0.5$ decreases continuously with increasing temperature, while at $x \geq 0.5$, it increases reaching minimum values due to the magnetic transition where the ferrimagnetic ordered state becomes paramagnetic disordered one [22]. In general the investigated samples are divided into two groups. Group 1 ($x \leq 0.5$) with negative S, indicating the semiconducting n-type behavior of the samples. Group II with positive S ($x \geq 0.5$)

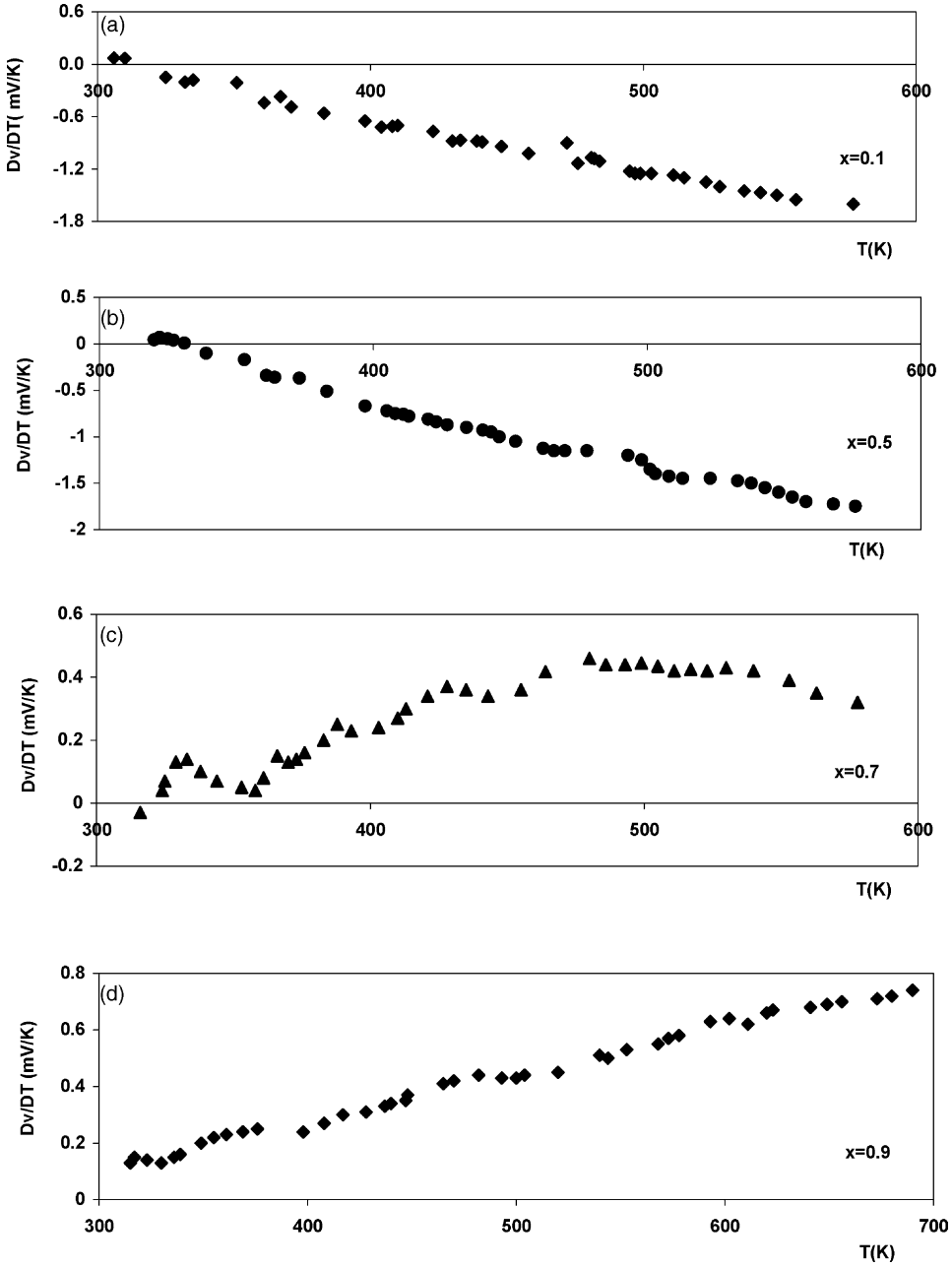

Fig. 6. (a–d) Variation of Seebeck coefficient (S) with absolute temperature (T) for $0.1 \leq x \leq 0.9$.

indicates the p-type behavior. The conduction mechanism in the n-type samples of group I is predominantly due to hopping of electron [23] from Fe^{2+} to Fe^{3+} ions ($Fe^{2+} \leftrightarrow Fe^{3+} + e^{-}$) whereas, the conduction mechanism in samples of group II can be explained on the basis of substituting Zn^{2+} ions for Fe^{3+} ions on the tetrahedral sites. This substitution might result in the formation of excess vacancies.

Fig. 7(a)–(d) shows the typical curve of XRD pattern of Zn substituted Li–La ferrite. The diffractograms show a (fcc) single phase spinel structure. The lattice parameter (a) is calculated from the experimental data and reported in Table 2. The variation of the lattice parameter (a) as a function of Zn addition (x) in the investigated samples is represented in Fig. 8; the figure shows that the lattice parameter decreases with increasing zinc content and lies in the expected range of spinel ferrites which agree well with JCPDS cards of Li–Zn ferrite (no. 1471). These results are explained on the fact that the presence of a small amount of Fe^{2+} on tetrahedral sites is sufficient enough to ionize Fe^{3+} ions at octahedral sites and the resulting electron is used by some Fe^{3+} ions.

Table 2
The value of the effective magnetic moment (μ_{eff}), Curie temperature (T_C), exchange interaction constant (J) and the lattice parameter (a) of $L_{i0.5-0.5x}Zn_xLa_yFe_{2.5-0.5x-y}O_4$

Zn content (x)	μ_{eff}			T_C (K)	J	a (A°)
	H = 2160 Oe	H = 3000 Oe	H = 3800 Oe			
0.1	3.92	3.46	2.56	913	314.99	8.345
0.5	4.03	3.91	3.81	693	239.09	8.339
0.7	4.11	3.98	3.51	673	232.19	8.335
0.9	3.67	3.44	2.89	823	283.94	8.425

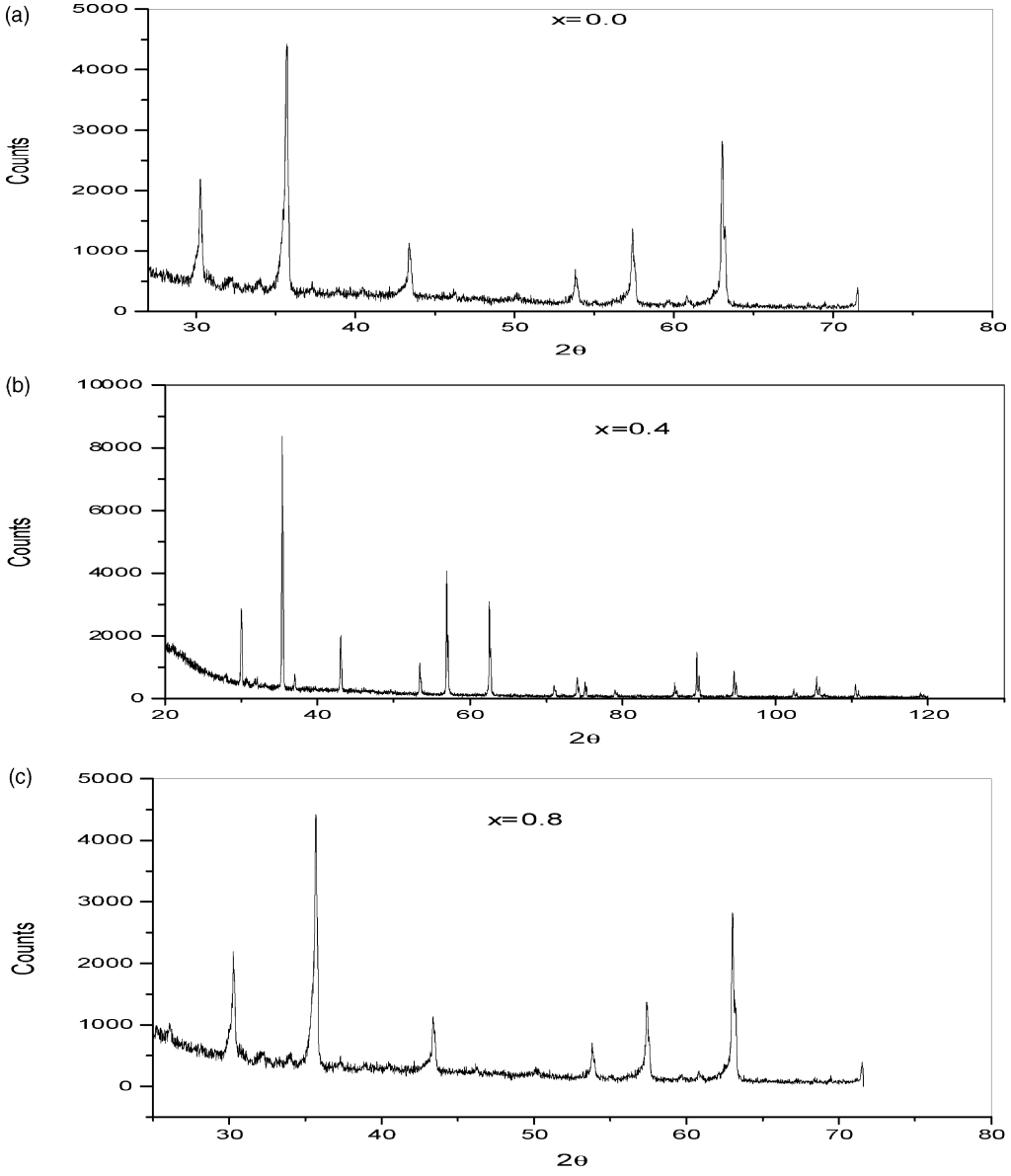

Fig. 7. X-ray diffraction pattern for $Li_{0.5-0.5x}Zn_xLa_yFe_{2.5-0.5x-y}O_4$; $0.1 \leq x \leq 0.9$.

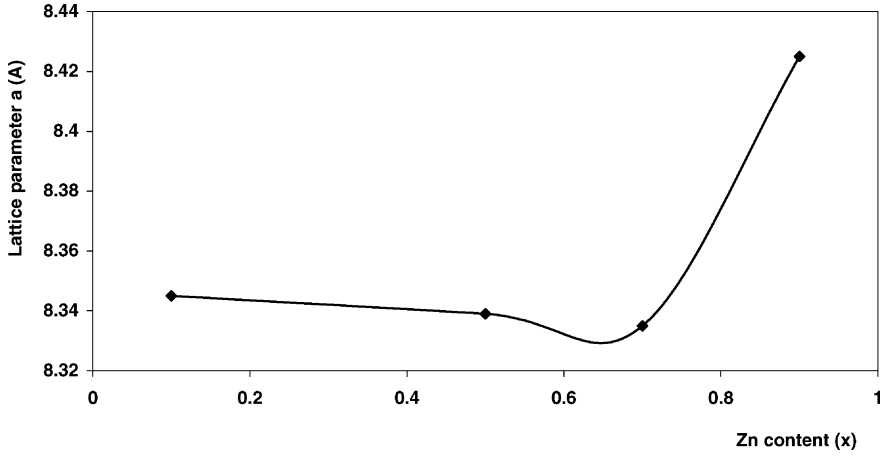

Fig. 8. The variation of lattice parameter (a) as a function of Zn content (x).

4. Conclusions

1. The dielectric constant (ε') of Li–Zn–La ferrite decreases with increasing frequency and decreases with increasing Zn content.
2. More than one straight line is obtained in the conductivity data intersecting at the Curie point indicating the presence of more than one conduction mechanism.
3. The small polaron hopping model of conductivity as well as the hopping of electrons are the most predominant processes.
4. The influence of rare earth (La^{3+}) ions is to decrease the magnetic interaction between A- and B-sites resulting in a decrease in the magnetic moment.
5. The negativity of thermoelectric power (n-type) decreases on increasing Zn^{2+} ions up to the critical concentration ($x = 0.5$) then Seebeck coefficient reverse its sign due to presence of holes (p-type).

References

[1] J. Smit, H.P.J. Wijn, Ferrite, John Wiley and Sons, 1965.
[2] B.K. Kumar, G.P. Srivastava, Proc. Int. Conf. Ferrites—India 5 (1989) 227.
[3] N.K. Grill, R.K. Puri, J. Mater. Sci. Lett. 4 (1985) 396.
[4] P.V. Reddy, M.B. Reddy, V.N. Muley, Y.V. Ramana, J. Mater. Sci. 7 (1988) 1243.
[5] A.A. Sattar, A.H. Wafik, H.M. El-Sayed, J. Phys. Stat. Sol. (a) 186 (3) (2001) 415.
[6] E. Rezlescu, C. Pasnicu, M.L. Craus, P.D. Popa, Cryst. Res. Technol. 31 (1996) 313.
[7] M.L. Crous, E. Rezlescu, N. Rezlescu, Phys. Stat. Sol. (a) 133 (1992) 439.
[8] E. Rezlescu, N. Rezlescu, C. Pasnicu, M.L. Craus, P.D. Popa, J. Mag. Mag. Mater. 117 (1992) 448.
[9] D. Ravinder, J. Phys. Stat. Sol. (a) 139 (1993) K69.
[10] P.V. Reddy, V.D. Reddy, D. Ravinder, J. Phys. Stat. Sol. (a) 127 (1991) 439.
[11] D. Ravinder, K.Vijaya Kumar, B.S. Boyanov, Mater. Lett. 38 (1999) 22.
[12] K.L. Yadav, R.N.P. Chowdhary, Mater. Lett. 19 (1994) 61.
[13] A.B. Naik, J.I. Power, Ind. J. Pure Appl. Phys. 23 (1985) 436.
[14] N. Rezlescu, D. Condurach, P. Petrariu, E. Luca, J. Am. Ceram. Soc. 57 (1974) 40.
[15] Pran Kishan, D.R. Sagar, Prem Swarup, J. Less Common Mater. 108 (1985) 345.
[16] M.I. Klings, J. Phys. C8 (1975) 3595.
[17] N. Rezlescu, D. Condurache, C. Naum, L. Luca, Rev. Roumaine Phys. 18 (1973) 727.
[18] K. Muraleedharan, J.K. Srivastava, V.R. Marathe, R. Vijayaraghavan, J.A. Kulkarni, V.S. Darsane, Solid State Commun. 55 (1985) 363.
[19] N. Rezlescu, E. Rezlescu, ICF 7 (1997) 225.
[20] B. Viswanathan, V.R.K. Murthy, Ferrite Materials Science and Technology, Narosa Publishing House, 1990.
[21] K. Latha, D. Ravinder, Phys. Stat. Sol. (a) 139K (1993) 109.
[22] Y. Purushotham, V.D. Reddy, D.R. Sagar, P. Kishan, P.V. Reddy, Phys. Stat. Sol. (a) 140 (1993) K89.
[23] A.N. Patil, R.P. Mahajan, K.K. Patankar, A.K. Ghatage, V.L. Mathe, S.A. Patil, Phys. Ind. J. Pure Appl. 38 (2000) 651.